International Journal of Conceptions on Mechanical and Civil Engineering
Vol. 6, Issue. 1, May' 2022; ISSN: 2357 – 2752

Parametric analysis of a solar air-heater roughened with multi-V ribs having trapezoidal slots

Swati Mor
Department of Mechanical Engineering
Amity University
Noida, Uttar Pradesh, India
swatimor.me@gmail.com

Niraj Kumar
Department of Mechanical Engineering
Amity University
Noida, Uttar Pradesh, India
nkumar21@amity.edu

B S Sikarwar
Department of Mechanical Engineering
Amity University
Noida, Uttar Pradesh, India
bssikarwar@amity.edu

Gulshan Sachdeva
Department of Mechanical Engineering
National Institute of Technology
Kurukshetra, Haryana, India
gulshansachdeva@nitkkr.ac.in

Abstract— **This paper presents a parametric study using ANSYS (ver.19.0) for a solar air-heater (SAH) roughened using multi-V ribs having trapezoidal slots. The computational results are drawn for Reynolds number (3000 to 15000), e/D_h (0.0258 to 0.056) and angle of attack (30° to 75°). The results from FLUENT of the present roughened geometry are compared with that of smooth duct. For the proposed roughness geometry, the optimum value of relative rib roughness (e/D_h) and angle of attack (α) obtained is 0.056 and 60° respectively at Reynolds number of 15,000. The maximum Nusselt number and friction factor for roughened geometry is found to be 142.6 and 0.033 respectively. For e/D_h=0.056, the maximum increment achieved for Nusselt number is 2.73, 2.91, 3.24 and 2.57 times at an angle of 30°, 45°, 60° and 75° respectively. While for relative roughness height of 0.056, the maximum increment obtained for friction factor is 2.04, 2.32, 2.55 and 1.87 times at an angle of 30°, 45°, 60° and 75° respectively.**

Keywords-Solar-air-heater (SAH); Multi-V ribs; Nusselt Number; Friction factor; CFD;

I. INTRODUCTION

The thermal energy transfer from the absorbing surface to the air in a solar air-heater is low and time dependent [1]. The formation of constant viscous layer at the absorber plate surface is responsible for the lower transfer of thermal energy. However, the viscous layer can be broken using artificial roughness which creates turbulence in air flow path and increase thermal energy transfer. Simultaneously, the roughness also contributes towards higher friction factor [2].

Roughness plays a crucial role in thermal energy transfer in a solar air-heater. Several investigators have worked over different types of roughness geometry to improve the performance of SAH [3-9]. Mahanand and Senapati [3] conducted the fluid flow and heat transfer analysis over a transverse inverted T-shaped ribbed absorber plate in a solar air-heater. In their study, they adopted RNG k-ε turbulence model for simulation and observed increment in thermal enhancement factor by 1.87 times of conventional SAH. Patel and Lanjewar [4] investigated the performance of solar air-heater roughened using V-ribs having symmetrical gap and staggered element. The maximum increment achieved in the value of Nusselt number and friction factor was 2.51 and 2.7 times that of conventional SAH for the ration of gap width to rib height of 1. Komolafe et al. [5] used rectangular ribs as artificial roughness over as absorber plate to enhance its efficacy. The maximum thermal efficiency obtained using this roughness geometry was 56.5% under the outdoor conditions. Both computational analysis and liquid crystal thermography (LCT) technique were adopted by Kumar and Layek [6] for analyzing the heat transfer distribution of transverse circular ribs in a SAH. The performance was tested for different Reynolds number ranging from 8551 to 11149 and for constant roughness pitch ratio of 10. Ghritlahre et al. [7] investigated the heat transfer rate in a solar air-heater roughened using arc-shaped ribs for the apex-up and apex-down air flow arrangement. The apex-up configuration was found to be more efficient than the apex-down air flow configuration for mass flow rate varying from 0.007 to 0.022 kg/s. Wang et al. [8] evaluated the thermal performance of solar air-heater roughened with S-shaped ribs having gap. The maximum thermal efficiency achieved using this roughness was 48%. Saravanan et al. [9] used the staggered multiple C-shaped perforated and non-perforated fins as roughness over absorber surface. The thermal performance of perforated C-shaped ribs was found to be slightly higher than that of non-perforated C-shaped ribs for relative height ratio of 0.6 and relative pitch to gap ratio of 3.8. Yadav and Bhagoria [10]

used RNG k- ε turbulence model to investigate the performance of twelve different configuration of square-sectioned transverse ribs in a SAH. It was reported that the maximum thermo-hydraulic performance using this roughness was found at e/D of 0.042 and P/e of 10.71. Kumar et al. [11] conducted experiment to test the performance of SAH for an arc-shaped wire rib arranged in S-shape over the surface of absorber plate. The maximum increment in Nusselt number and friction factor was observed at p/e of 8, e/D_h of 0.043 and arc angle of 60˚. Hans et al. [12] derived a correlation for friction factor and heat transfer in terms of flow and roughness geometry parameters for broken arc ribs as artificial roughness. In this study, the experimental results of the broken arc ribs were compared with that of smooth duct and continuous arc-shaped ribs. Two-dimensional simulation study was conducted by Gawande et al. [13] using ANSYS fluent in a SAH roughened with reverse L-shaped ribs. The thermohydraulic performance factor of 1.90 was achieved using this roughness geometry. A square wave profiled transverse ribs were used as roughness geometry by Singh et al. [14] for analyzing its performance. The thermal efficiency of non-uniform ribs was compared with that of uniform ribbed transverse ribs. Kumar and Layek [15] experimented over a twisted rib roughened solar air heater to find a correlation for friction factor and Nusselt number. The results were drawn for rib inclination angle ranging from 30˚ to 90˚ and twist ratio varying from 3 to 7. Deo et al. [16] investigated the flow characteristics of air in a solar air-heater roughened with multigap V-down ribs. The maximum value of Nusselt number obtained was 3.34 times that of smooth duct at Re=12000.

Several studies were attempted to investigate the heat transfer characteristics of various types of artificial roughness pattern [11-16]. However, no work done on multi-V ribs having trapezoidal slots. To increase the secondary heat transfer zone, trapezoidal slots are provided in the V-shaped ribs which give more surface area to the flowing air and enhance the thermal transfer rate.

II. COMPUTATIONAL DOMAIN

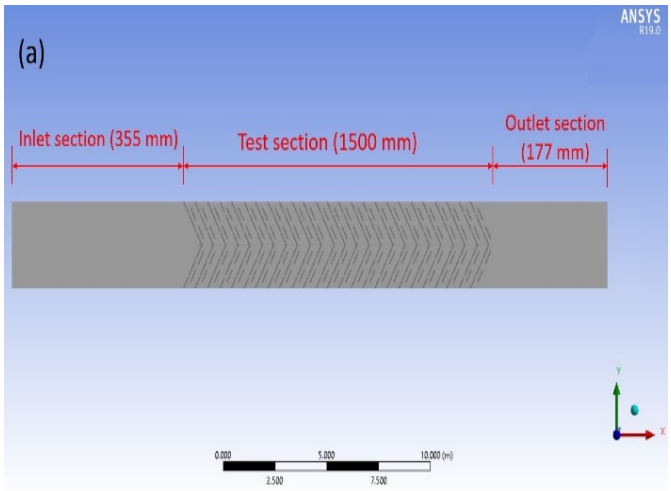

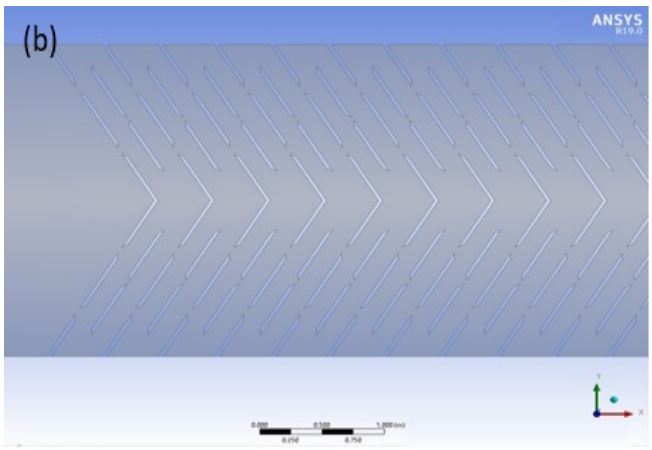

Figure 1. (a) Solar air-heater model with multi-V ribs having trapezoidal slot (both sides slanted at an angle of 60˚) in ANSYS design modeler (b) Detailed view of test section in a SAH

The geometry is modelled using ANSYS design modeler by defining the computational domain in form of smooth duct and proposed roughened duct respectively. The rectangular duct consists of inlet region, test region and outlet region of length 355 mm, 1500 mm and 177 mm respectively as shown in fig.1. The duct is divided into three regions maintaining the ASHRAE 93-2003 standards [17]. The test region of the solar air-heater is roughened using multi-V ribs having trapezoidal slot having geometrical parameters of different values as shown in table I.

TABLE I. GEOMETRICAL PARAMETERS OF A SOLAR AIR-HEATER USED FOR SIMULATION

S.No.	Parameters	Range of values
1	Relative staggered rib pitch (p/P)	0.62
2	No. of gaps (n)	2
3	Relative roughness height (e/D_h)	0.0258 -0.056 (4 levels)
4	Angle of attack (α)	30˚- 80˚
5	Angle of inclination (Trapezoidal slot)	60˚
6	Relative roughness pitch (P/e)	10
7	Reynolds number (Re)	3000 – 15000 (5 levels)

Assumptions made while conducting the simulation analysis:
a) The initial temperature considered is 300 K.
b) The heated plate receives the heat flux of 1000 W/m^2 while the other walls are considered to be insulated.
c) Thermo-physical properties are assumed to be constant for adiabatic walls, working fluid and heated plate.
d) The fluid flow is fully developed throughout the test region of the solar air-heater.
e) Radiation effect is not considered.

III. GOVERNING EQUATIONS

The behaviour of the fluid flow inside the solar air-heater is governed by various equations in form of RANS based Navier Stokes equation [18] given by

Conservation of mass:

$$\frac{\partial(\rho u_j)}{\partial x_j} = 0 \quad (1)$$

Conservation of momentum:

$$\frac{\partial}{\partial x_j}(\rho u_i u_j) = -\frac{\partial P}{\partial x_i} + \frac{\partial}{\partial x_j}\left[(\mu + \mu_t)\left(\frac{\partial u_i}{\partial x_j} + \frac{\partial u_j}{\partial x_i}\right)\right] \quad (2)$$

Conservation of energy:

$$\frac{\partial}{\partial x_i}(u_i T) = \frac{\partial}{\partial x_i}\left[\left(\frac{\mu}{Pr} + \frac{\mu_t}{Pr_t}\right)\frac{\partial T}{\partial x_j}\right] \quad (3)$$

where ρ, α and μ represents density, thermal conductivity and viscosity of the working fluid respectively

The transport equation used in RNG k-ε turbulent model is given by

$$\frac{\partial}{\partial x_i}(\rho k u_i) - \frac{\partial}{\partial x_j}\left(\alpha_k \mu_{eff}\frac{\partial k}{\partial x_j}\right) = G_k - \rho\varepsilon \quad (4)$$

$$\frac{\partial}{\partial x_i}(\rho\varepsilon u_j) - \frac{\partial}{\partial x_j}\left(\alpha_\varepsilon \mu_e \frac{\partial \varepsilon}{\partial x_j}\right) = C_{1\varepsilon}\frac{\varepsilon}{k}G_k - C_{2\varepsilon}\rho\frac{\varepsilon^2}{k} - R_\varepsilon \quad (5)$$

$$\mu_{eff} = \mu_f + \mu_t = \mu_t + \rho C_\mu \frac{k^2}{\varepsilon} \quad (6)$$

where G_k and μ_{eff} represents production term and effective viscosity while α_k, α_ε, $C_{1\varepsilon}$, C_μ, and $C_{2\varepsilon}$ are constant.

IV. Grid Independence Test

Grid independence test is applied to evaluate the fineness and mesh size of the developed fluid domain model. The main purpose of this test is to identify the number of element size at which the results become independent of the mesh element. For present study, the computational domain is discretized using non-uniform structured grids. The boundary walls of the roughness geometry are fined using inflation method. Table II shows the grid independence test of the present duct at Re=15000. The simulated results are taken for Nusselt number at different face size. It is found that Nusselt number values is almost constant after 3,87,346 no. of elements. So, the most suitable condition for obtaining the exact value of Nusselt number is at 3,87,346 no. of elements.

TABLE II. VARIATION OF AVERAGE NUSSELT NUMBER WITH NUMBER OF COMPUTATIONAL CELLS

S.No.	Number of cells	Nusselt number	% Variation in Nusselt number
1	2,34,345	131.5124	-
2	2,98,564	134.2740	2.8
3	3,43,256	139.7341	2.3
4	3,87,346	142.0643	0.9
5	4,43,323	142.8562	0.5

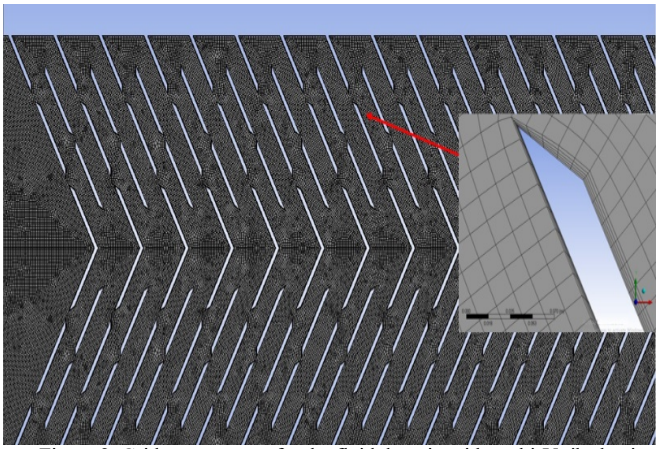

Figure 2. Grid arrangement for the fluid domain with multi-V ribs having trapezoidal slots roughened absorber plate

V. Turbulence Model Validation

In present study, the turbulence model adopted is RNG k-ε model along with enhanced wall treatment [19, 20]. The turbulence model is validated using the correlation for Nusselt number and friction factor by using Dittus-Boelter and Blasius equation respectively.

$$Nu = 0.024\ Re^{0.8}\ Pr^{0.4} \quad (1)$$

$$C_f = 0.085\ Re^{-0.25} \quad (2)$$

As shown in fig.3 and fig.4, the CFD results of the smooth duct show good agreement with the empirical relation. Thus, it marks the validation of the present turbulence model for further study of the proposed roughened duct.

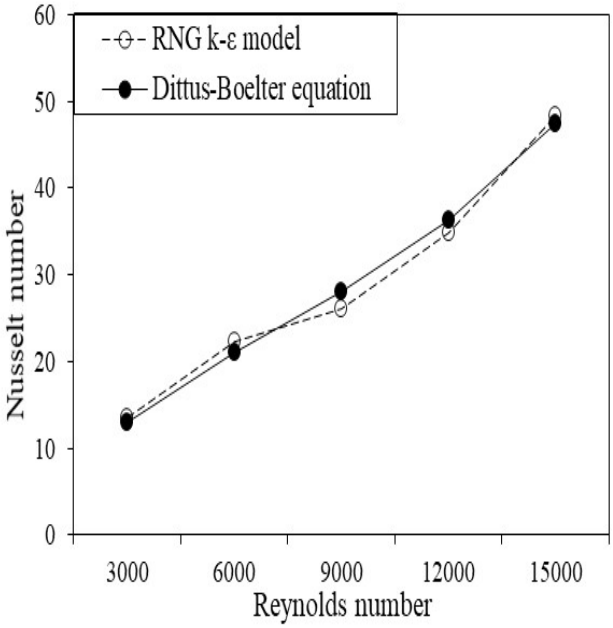

Figure 3. Validation of Nusselt number

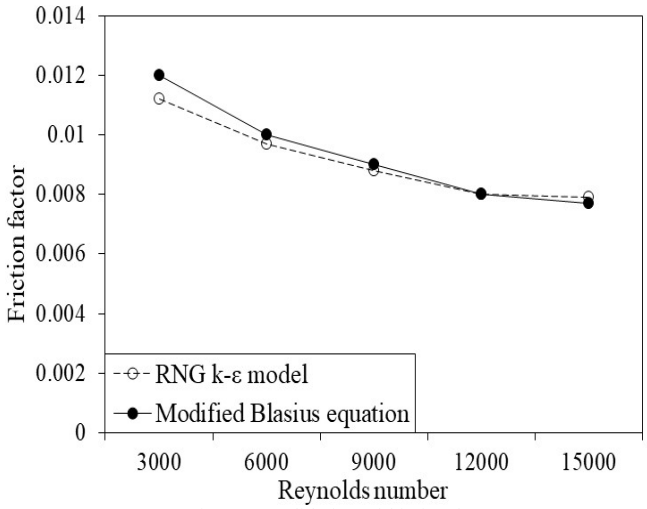

Figure 4. Validation of friction factor

VI. RESULT AND DISCUSSION

A. Effect of angle of attack (α)

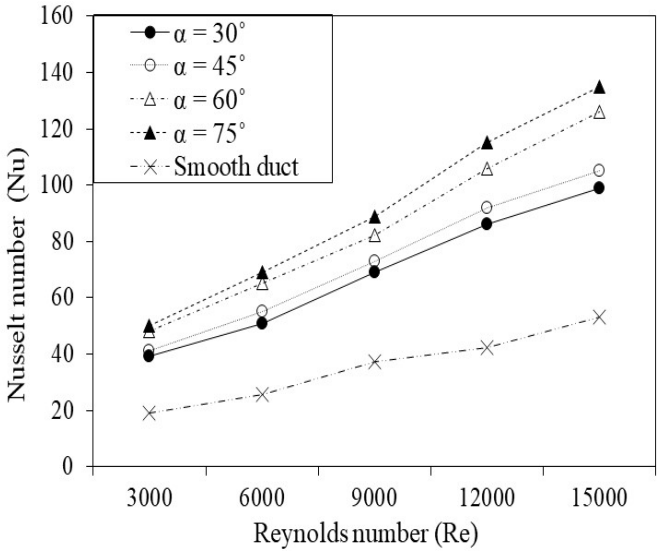

Figure 5. Variation of Nusselt number at different α

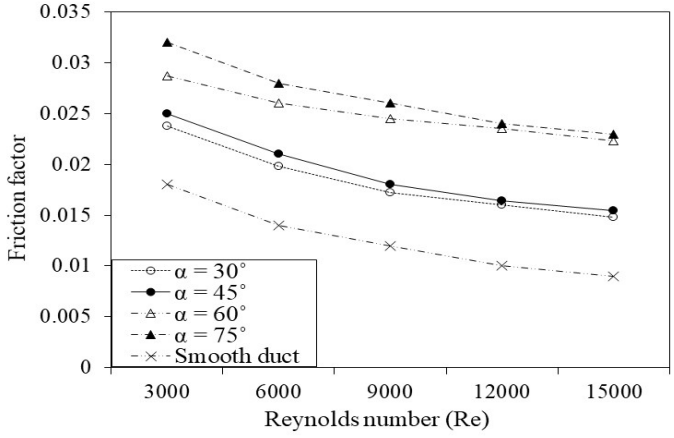

Figure 6. Variation of friction factor at different α

Angle of attack (α) has significant effect over the performance of solar air heater as optimum angle of attack provides better transfer of thermal energy from the absorbing surface to the air. Fig.5 shows the Nusselt number variation for different angle of attack ranging from 30˚ to 90˚ at different Reynolds number.

The increment in Nusselt number value is found to be maximum at angle of attack of 60˚. After 60˚ angle of attack, the increment in Nusselt number value starts declining until it reaches 90˚. The secondary flow formation at angle of attack of 60˚ is maximum and uniformly distributes the fluid flow through the duct. Fig.6 shows the variation of friction factor at different angle of attack. It is found that 60˚ angle of attack contributes to lesser frictional loss increment. So, to take the maximum benefit of multi-V ribs having trapezoidal slot, the best orientation is at angle of 60˚.

B. Effect of relative roughness height (e/D_h)

The value of Nusselt number is plotted at different Reynolds number varying from 3000 to 15000 and for different values of e/D_h = 0.0258, 0.034, 0.043 and 0.056 as shown in fig.7. It is visible from fig.6 that increase in e/D_h value contribute towards enhanced thermal energy transfer because of improved turbulence kinetic energy. Along with increased thermal energy, the artificial roughness also contributes towards considerable friction factor, thus, the effect of e/D_h over the value of friction loss need to be investigated.

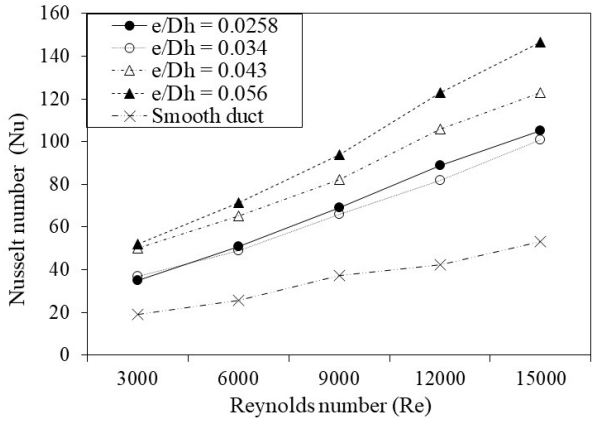

Figure 7. Variation of Nusselt number at different e/D_h

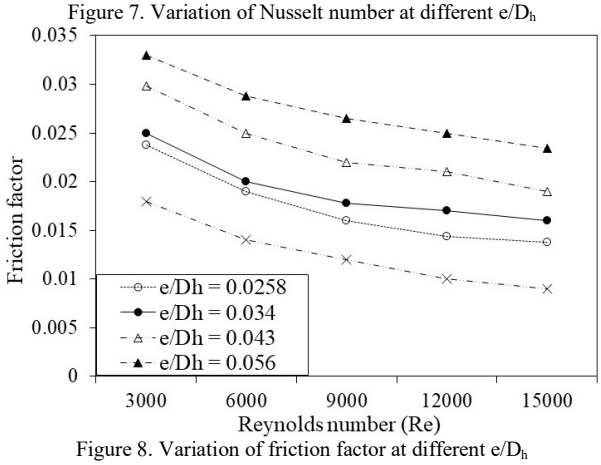

Figure 8. Variation of friction factor at different e/D_h

Fig.8 shows the effect of e/D_h over the friction factor value. It is evident that the flow resistance increases with increase in e/D_h. So, increment in e/D_h contributes to increase in Nusselt number as well as friction factor. Hence, it is crucial to select an optimum value of e/D_h at which there is balance in increment of Nusselt number and decrement of friction factor.

C. Effect of trapezoidal slot in multi-V ribs

Broken ribs help in breakdown of laminar viscous layer and create turbulence, ultimately leading to enhanced thermal energy transfer. Increased number of gaps in artificial roughness geometry leads to vortices generation near the gaps, which further increases the thermal energy transfer regions inside the duct.

The trapezoidal slots in multi-V ribs give rise to the secondary flow which accelerates the main flow inside the solar air heater. The increase area due to presence of trapezoidal slots improves the boundary layer flow and hence, higher air temperature is achieved at outlet for present geometry as compared to multi-V ribs with gaps. Fig.9 and fig.10 shows the temperature contours and velocity contours of solar air-heater roughened with multi-V ribs having trapezoidal slot at Re=15000.

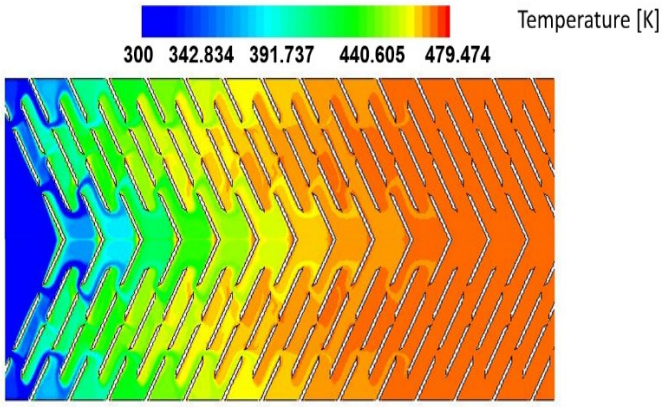

Figure 9. Temperature contours for absorber surface with multi-V ribs having trapezoidal slot (e/D_h =0.043, P/e= 10 and Re = 15,000)

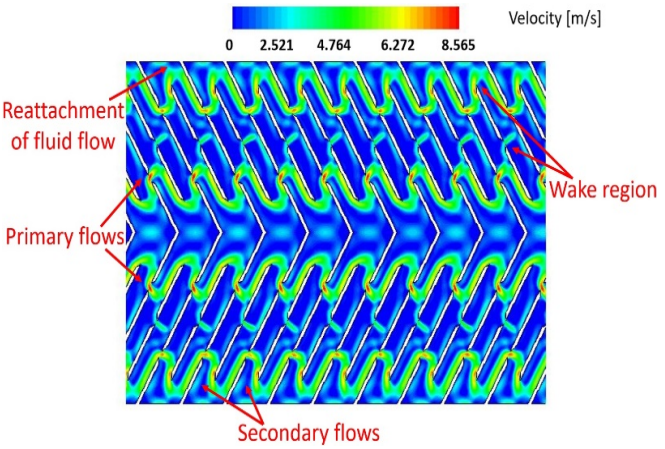

Figure 10. Velocity contours of SAH with multi-V ribs having trapezoidal slot (e/D_h =0.043, P/e= 10 and Re = 15,000)

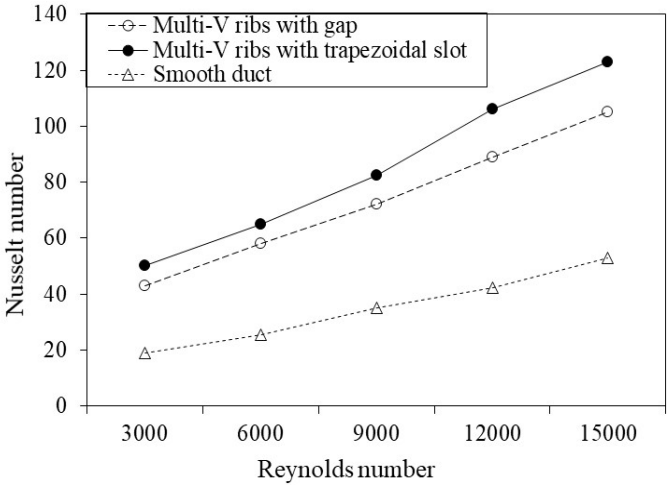

Figure 11. Variation of Nusselt number with respect to Reynolds number

Fig.11 shows that maximum increment in Nusselt number is obtained for multi-V ribs having trapezoidal slots. Also, maximum value of friction factor is obtained for present geometry as compared to multi-V ribs with gaps and smooth duct, shown by fig.12.

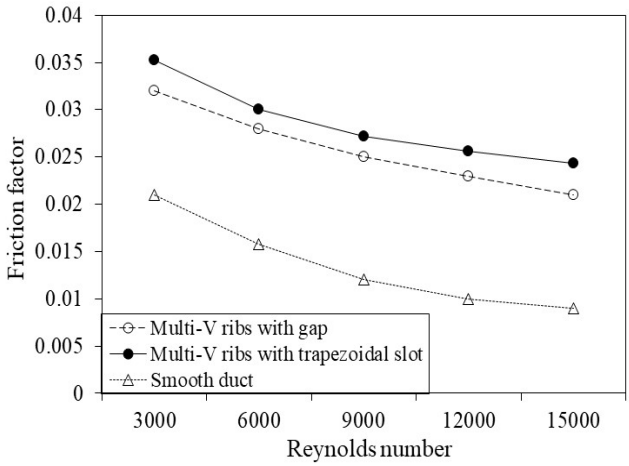

Figure 12. Variation of friction factor with respect to Reynolds number

VII. CONCLUSIONS

In present study, the effect of presence of multi-V ribs having trapezoidal slots over the thermal energy transfer capacity of solar air-heater is investigated. Result shows that multi-V ribs having trapezoidal slots show increment in Nusselt number by 1.46 times that of the multi-V ribs having gap, due to increase in number of thermal energy transfer regions.

Before doing comparative analysis, a numerical study is done to investigate the optimum geometrical parameters of the present roughness pattern at which thermal efficiency of the SAH is maximum. The optimum value of relative rib roughness (e/D_h) and angle of attack (α) obtained is 0.056 and 60° respectively at Reynolds number of 15,000. For e/D_h=0.056, the maximum increment achieved in value of Nusselt number 2.73, 2.91, 3.24 and 2.57 times at an angle of

30˚, 45˚, 60˚ and 75˚ respectively. While for relative roughness height of 0.056, the maximum increment in value of friction factor is 2.04, 2.32, 2.55 and 1.87 times at an angle of 30˚, 45˚, 60˚ and 75˚ respectively.

REFERENCES

[1] P.T. Saravanakumar, D. Somasundaram and M.M. Matheswaran, "Thermal and thermo-hydraulic analysis of arc shaped rib roughened solar air heater integrated with fins and baffles", Sol. Energy, vol. 180, pp. 360-371, 2019.

[2] M.K. Sahu and R.K. Prasad, "Thermohydraulic performance analysis of an arc shape wire roughened solar air heater", Renew. Energy, vol. 108, pp. 598-614, 2017.

[3] Y. Mahanand and J.R. Senapati, "Thermal enhancement study of a transverse inverted-T shaped ribbed solar air heater", Int. Commun. Heat Mass Transf., vol. 119, pp. 104922, 2020.

[4] S.S. Patel and A. Lanjewar, "Heat transfer enhancement using additional gap in symmetrical element of V-geometry roughened solar air-heater", J. Energy Storage, vol. 38, pp. 102545, 2021.

[5] C.A. Komolafe, I.O. Oluwaleye, O. Awogbemi and C.O. Osueke, "Experimental investigation and thermal analysis of solar air heater having rectangular rib roughness on the absorber plate", Case Studies Therm. Eng., vol. 14, pp. 100442, 2019.

[6] A. Kumar and A. Layek, "Nusselt number and fluid flow analysis of solar air heater having transverse circular rib roughness on absorber plate using LCT and computational technique", Thermal Sci. Eng. Progress, vol. 14, pp. 100398, 2019.

[7] H.K. Ghritlahre, P.K. Sahu and S. Chand, "Thermal performance and heat transfer analysis of arc shaped roughened solar air heater – An experimental study", Sol. Energy, vol. 199, pp. 173-182, 2020.

[8] D. Wang et al., "Evaluation of the performance of an improved solar air heater with "S" shaped ribs with gap", Sol. Energy, vol. 195, pp. 89-101, 2020.

[9] A. Saravanan at al., "Thermo-hydraulic performance of a solar air heater with staggered C-shape finned absorber plate", Int. J. Therm. Sci., vol. 168, pp. 107068, 2021.

[10] A.S. Yadav and J.L. Bhagoria, "A numerical investigation of square sectioned transverse rib roughened solar air heater", Int. J. Therm. Sci., vol.79, pp. 111-131, 2014.

[11] K. Kumar, D.R. Prajapati and S. Samir, "Heat transfer and friction factor correlations development of solar air heater duct artificially roughened "S" shape ribs", Expt. Therm. Fluid Sci., vol.82, pp. 249-261, 2017.

[12] V.S. Hans, R.S. Gill and S. Singh, "Heat transfer and friction factor correlations for a solar air heater duct roughened artificially with broken arc ribs", Expt. Therm. Fluid Sci., vol.80, pp.77-89, 2017.

[13] V.B. Gawande, A.S. Dhoble, D.B. Zodpe and S. Chamoli, "Experimental and CFD investigation of convection heat transfer in solar air heater with reverse L-shaped ribs", Sol. Energy, vol. 131, pp. 275-295, 2016.

[14] I. Singh, S. Vardhan, S. Singh and A. Singh, "Experimental and CFD analysis of solar air heater duct roughened with multiple broken transverse ribs: A comparative study", Sol. Energy, vol. 188, pp. 519–532, 2019.

[15] A. Kumar and A. Layek, "Nusselt number and friction factor correlation of solar air heater having twisted-rib roughness on absorber plate", Renew. Energy, vol. 130, pp. 687-699, 2018.

[16] N.S. Deo, S. Chander and J.S. Saini, "Performance analysis of solar air heater duct roughened with multigap V-down ribs combined with staggered ribs", Renew. Energy, Vol.91, pp. 484-500, 2016.

[17] ASHRAE Standard 93-77, "Method of testing to determine the thermal performance of solar air-heater", New York, pp. 1-34, 1977.

[18] G. Xie, J. Liu, P.M. Ligrani and W. Zhang, "Numerical analysis of flow structure and heat transfer characteristics in square channels with different internal-protruded dimple geometrics", Int. J. Num. Methods Heat Fluid flow, vol. 67, pp. 81-97, 2013.

[19] V.B. Gawande, A.S. Dhoble, D.B. Zodpe and S. Chamoli, "Experimental and CFD investigation of convection heat transfer in solar air heater with reverse L-shaped ribs", Sol. Energy, vol. 131, pp. 275-295, 2016.

[20] Y. Mahanand and J.R. Senapati, "Thermal enhancement study of a transverse inverted-T shaped ribbed solar air heater", Int. Comm. Heat Mass Transf., vol. 119, pp. 104922, 2020